Interannual Variability of the Atlantic Hadley Circulation in Boreal Summer and Its Impacts on Tropical Cyclone Activity

GAN ZHANG AND ZHUO WANG

Department of Atmospheric Sciences, University of Illinois at Urbana–Champaign, Urbana, Illinois

(Manuscript received 16 November 2012, in final form 22 May 2013)

ABSTRACT

A novel method was developed to define the regional Hadley circulation (HC) in terms of the meridional streamfunction. The interannual variability of the Atlantic HC in boreal summer was examined using EOF analysis. The leading mode (M1), explaining more than 45% of the variances, is associated with the intensity change of the ITCZ. M1 is significantly correlated to multiple climate factors and has strong impacts on Atlantic tropical cyclone (TC) activity. In the positive (negative) phase of M1, the ITCZ is stronger (weaker) than normal, and more (fewer) TCs form over the main development region (MDR) with a larger (smaller) fraction of storms intensifying into major hurricanes. Analyses showed that the large-scale dynamic and thermodynamic conditions associated with a stronger ITCZ are more favorable for TC activity.

The roles of tropical easterly waves in modulating the Atlantic TC activity are highlighted. In the positive phase of M1, the wave activity is significantly enhanced over the MDR and the Caribbean Sea, which can be attributed to stronger coastal convection and mean flow structure changes. In the context of the recently proposed marsupial paradigm, the frequency and structure of wave pouches were examined. In the positive phase of M1, the pouch frequency increases, and the number of pouches with a vertically coherent structure also rises significantly. A deep and vertically aligned wave pouch has been shown to be highly favorable for TC formation.

The HC perspective thus unifies both dynamic and thermodynamic conditions impacting Atlantic TC activity and helps explain the statistical linkages between Atlantic TC activity and different climate factors.

1. Introduction

The Hadley circulation is one of the primary components of the large-scale circulation in the tropics. It consists of two thermally direct overturning cells in which air rises near the equator, diverts poleward near the tropopause, descends in the subtropics, and returns equatorward near the surface. Because of the Coriolis force, the upper-level poleward flow turns eastward and contributes to the subtropical westerly jet. Similarly, the equatorward flow turns westward and results in the prevailing trade winds in the lower troposphere. The northeasterly and southeasterly trade winds meet in the intertropical convergence zone (ITCZ). Associated with the ascending branch of Hadley cells, the ITCZ is featured by heavy precipitation, cyclonic relative vorticity, and relatively low surface pressure. The variability of the Hadley circulation is thus closely related to different aspects of the tropical climate, such as precipitation distribution, low-level convergence and relative vorticity, as well as tropospheric humidity and vertical wind shear (VWS).

The intensity of globally averaged Hadley circulation is significantly modulated by the variations of the El Niño–Southern Oscillation (ENSO) on the interannual time scale (Oort and Yienger 1996). Recent work suggests an intensifying trend of the Hadley circulation in the past three decades (e.g., Mitas and Clement 2005; Stachnik and Schumacher 2011). Chiang et al. (2002) examined the interannual variability of the Atlantic ITCZ precipitation and suggested that the variability is mainly controlled by the meridional sea surface temperature (SST) gradient of the tropical Atlantic and the anomalous Walker circulation associated with ENSO. The meridional SST gradient is linked to the Atlantic meridional mode (AMM; Chiang and Vimont 2004), which is associated with the meridional displacement of the ITCZ.

The impacts of the large-scale circulation on Atlantic tropical cyclone (TC) activity have been examined in

Corresponding author address: Zhuo Wang, University of Illinois at Urbana–Champaign, Department of Atmospheric Sciences, 105 South Gregory St., Urbana, IL 61801.
E-mail: zhuowang@illinois.edu

DOI: 10.1175/JCLI-D-12-00802.1

many previous studies. Shapiro (1982) showed that the lower large-scale sea level pressure and weaker 500-hPa westerlies over the North Atlantic precede more active hurricane seasons. Gray (1984a) highlighted the impacts of ENSO on the Atlantic TC frequency via changes of the upper-level flow pattern and the associated VWS. Landsea and Gray (1992) and Gray and Landsea (1992) found a significant correlation between the June–September rainfall in the western Sahel and the number of intense hurricanes, and hypothesized that the enhanced TC activity is due to the weaker VWS and stronger African easterly waves (AEWs) in a wet year. Goldenberg et al. (2001) investigated the interannual and interdecadal variability of the TC activity over the main development region (MDR) and suggested that greater hurricane activity in 1995–2000 can be attributed to the simultaneous increases in North Atlantic SST and decreases in VWS. Vimont and Kossin (2007) and Kossin and Vimont (2007) showed that the AMM is correlated with local dynamical and thermodynamic variables, such as SST, VWS, and static stability, which cooperatively impact Atlantic TC activity.

Over the Atlantic, a majority of TCs originate from AEWs (Landsea 1993). The relationship between AEW activity and TC activity over the Atlantic has been examined in some previous studies. Reed (1988) suggested that TC activity may be related to the variability of AEW intensity. Thorncroft and Hodges (2001) showed a positive correlation between Atlantic TC activity and the 850-hPa wave activity at the West African coast, which was further confirmed by Hopsch et al. (2007). Most of these studies, however, mainly focused on waves over West Africa. The structure and variability of tropical easterly waves (TEWs) over the Atlantic and their relationship with TC activity are not well understood.

Recent work by Dunkerton et al. (2009) showed that a region of cyclonic recirculation exists in the lower troposphere in some, but not all, easterly waves. Such a region, the so-called wave pouch, straddles the ''critical latitude'' where the wave phase speed and mean flow speed are equal. As demonstrated by both observational diagnoses (Wang et al. 2009; Raymond and López Carrillo 2011) and numerical model simulations (Wang et al. 2010a,b; Wang 2012; Montgomery et al. 2010; Fang and Zhang 2010), a wave pouch can protect a protovortex inside from strain/shear deformation and dry air intrusion above the boundary layer, and its cyclonic gyre also provides a focal point for vorticity aggregation. Wang et al. (2012) further examined the vertical structure of wave pouches and suggested that a moist and convectively active wave pouch extending from the middle troposphere (600–700 hPa) down to the boundary layer is a necessary and highly favorable condition for TC formation. The marsupial paradigm provides a new perspective to examine the impacts of the large-scale circulation on TC formation.

In summary, Atlantic TC activity is controlled by multiple factors—local and remote, dynamic and thermodynamic, from the basin scale to the synoptic scale. Although different studies emphasized different aspects, these factors are not independent of each other (e.g., Emanuel 2007). To better understand the variability and predictability of Atlantic tropical cyclone activity, we need to understand how the variabilities of different environmental factors are linked to each other and how they are controlled by the local and remote SST forcing. In this study we will examine the variability of the Atlantic Hadley circulation and its impacts on TC activity. As the study will show, the Hadley circulation links various aspects of the large-scale circulation and provides a useful framework to understand the physical linkage between the large-scale circulation and Atlantic TC activity. Using insights from the marsupial paradigm, we will also examine tropical easterly waves as a ''connecting link'' between the large-scale circulation and TC development.

The remainder of the paper is organized as follows. The data and methodology are described in section 2. The interannual variability of the Atlantic Hadley circulation is presented and discussed in section 3. The impacts of the interannual variability of the Atlantic Hadley circulation on TC activity are examined in section 4, followed by a summary and discussion in section 5.

2. Data and methodology

a. Data

Monthly mean wind data from the National Centers for Environmental Prediction (NCEP)–Department of Energy (DOE) Reanalysis 2 (NNR2; Kanamitsu et al. 2002) were used to derive the meridional streamfunction (defined in section 2b) and examine the large-scale atmosphere circulation, and the 6-h data from NNR2 were used to investigate the TEW activity. A 2.5–9-day bandpass filter and a 2.5-day low-pass filter were constructed (Doblas-Reyes and Déqué 1998) and applied to the 6-h wind data. The former was used to extract the tropical easterly waves, and the latter was used to remove the high-frequency fluctuations. The low-pass filtered data can be regarded as the sum of the mean flow and wave perturbations. Monthly SST data from the NOAA Extended Reconstructed Sea Surface Temperature, version 3b (ERSST; Xue et al. 2003; Smith et al. 2008), and monthly precipitation data from the Global Precipitation Climatology Project (GPCP; Adler et al.

2003) were also used in this study. GPCP was selected since it represents the oceanic precipitation more reasonably than the Climate Prediction Center (CPC) Merged Analysis of Precipitation (CMAP) does (Yin et al. 2004). The North Atlantic hurricane database (HURDAT; Landsea et al. 2008), also known as the best-track data, was used to examine the TC activity, including genesis, storm tracks, and intensity. The MDR SST is defined here as the average over 10°–20°N, 20°–70°W, and the relative SST index is defined as the difference of the MDR SST and the tropical global (20°S–20°N) mean SST. The Atlantic equatorial mode (AEM) index was represented with the regionally average SST (4°S–4°N, 20°W–0°), similar to Zebiak (1993), derived from ERSST. Time series of other climate indices, if not specified otherwise, were downloaded from the NOAA/Physical Sciences Division (PSD; http://www.esrl.noaa.gov/psd/data/climateindices/list/) and used to examine the linkage between different climate factors and the Atlantic Hadley circulation. Our study mainly focuses on July–September (JAS) in the Atlantic hurricane season, owing to the significant change of the large-scale circulation in October. October is briefly discussed in section 4c.

b. Methodology

The Stokes streamfunction has been commonly used to study the mean meridional circulation (e.g., Oort and Rasmusson 1970; Oort and Yienger 1996; Dima and Wallace 2003). In this approach, the meridional circulation was assumed to be nondivergent, that is, $\partial v/\partial y + \partial \omega/\partial p = 0$, so there is no net mass flux in the zonal direction. A streamfunction can thus be defined for the meridional circulation (Oort and Yienger 1996), which satisfies

$$[\overline{v}] = g\frac{\partial \psi}{2\pi R\cos\phi \partial p} \quad \text{and} \tag{1}$$

$$[\overline{\omega}] = -g\frac{\partial \psi}{2\pi R^2\cos\phi \partial \phi}, \tag{2}$$

where v is the meridional velocity, ω is the vertical velocity in pressure coordinates, ψ is the Stokes streamfunction in spherical coordinates, R is the mean radius of the earth, ϕ is latitude, and the overbars and brackets denote temporal and zonal averaging, respectively. The Stokes streamfunction is often derived by vertical integration of the meridional wind based on Eq. (2):

$$\psi = \frac{2\pi R}{g}\int [\overline{v}]\cos\phi \, dp. \tag{3}$$

The assumption of nondivergent meridional circulation is valid over the global domain, but it breaks down over regional domains when the net zonal mass transport of the domain is not negligible. To study the variability of the Atlantic Hadley circulation, we took a novel approach to define the streamfunction. The horizontal wind field can be decomposed into the nondivergent and irrotational components, and only the irrotational component contributes to the vertical motion. The irrotational component of the meridional flow can be regarded as part of the north–south overturning circulation, that is, the Hadley circulation, and the irrotational component of the zonal flow can be regarded as part of the east–west overturning circulation, that is, the Walker circulation. We can thus divide the vertical velocity into two parts, one associated with the Hadley circulation and one with the Walker circulation:

$$\frac{\partial v_\chi}{\partial y} + \frac{\partial \omega_H}{\partial p} = 0 \quad \text{and} \tag{4}$$

$$\frac{\partial u_\chi}{\partial x} + \frac{\partial \omega_W}{\partial p} = 0, \tag{5}$$

where the subscript χ denotes the irrotational wind component, the subscripts H and W denote the Hadley circulation and the Walker circulation; the sum of ω_H and ω_W yields the total vertical motion. Note that such partitioning does not imply that the zonal and meridional circulations are independent of each other. The coupling of zonal and meridional circulations has been suggested as being responsible for the interbasin association (e.g., Chang et al. 2000; Chiang et al. 2002).

Using Eq. (4), the meridional streamfunction for the Hadley circulation can be derived based on the irrotational component of the meridional flow:

$$\psi = \frac{2\pi R}{g}\int [v_\chi]\cos\phi \, dp, \tag{6}$$

where downward integration was applied by assuming $\psi = 0$ at the top of the atmosphere. To study the interannual variability of the Hadley circulation over the Atlantic, the JAS seasonal mean meridional wind was averaged over 20°–70°W to derive the streamfunction. Empirical orthogonal function (EOF) and composite analyses were then used to extract the dominant modes of the interannual variability and examine their impacts on TCs.

3. Variability of the Hadley circulation

a. Meridional streamfunction analysis

The JAS mean meridional streamfunction over the Atlantic averaged over 1979–2010 is shown in Fig. 1a.

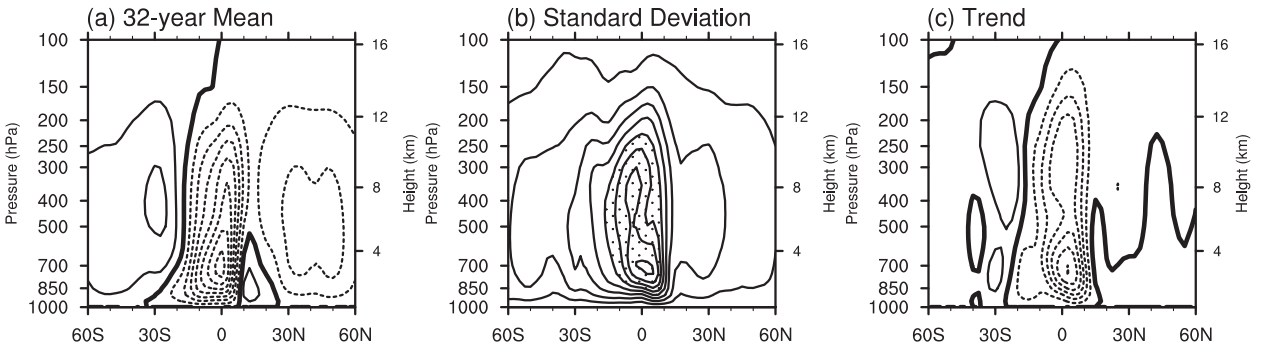

FIG. 1. (a) The 32-yr mean, (b) standard deviation, and (c) 32-yr trend of the JAS seasonal mean streamfunction. Zero lines are thickened in (a) and (c), and solid (dashed) lines indicate positive (negative) values; values greater than $2.5 \times 10^{10}\,\mathrm{kg\,s^{-1}}$ are stippled in (b). Contour intervals are $0.3 \times 10^{11}\,\mathrm{kg\,s^{-1}}$, $0.5 \times 10^{10}\,\mathrm{kg\,s^{-1}}$, and $0.5 \times 10^{9}\,\mathrm{kg\,s^{-1}\,yr^{-1}}$ in (a)–(c), respectively.

There are four circulation cells between 60°S and 60°N. The most prominent cell is the southern Hadley cell, with the upward motion slightly north of the equator and the downward motion around 15°S. The amplitude of the streamfunction associated with this cell is about $-2.2 \times 10^{11}\,\mathrm{kg\,s^{-1}}$, comparable to the global average reported in previous studies (e.g., Oort and Yienger 1996; Dima and Wallace 2003; Mitas and Clement 2005; Stachnik and Schumacher 2011). The northern Hadley cell is much weaker in amplitude and has a shallower vertical structure. The asymmetry of the Hadley circulation between the winter and summer hemispheres can be attributed to the weak inertial stability equatorward of the ITCZ (Hack et al. 1989). Farther poleward of the Hadley cells are the so-called Ferrel cells, with subsidence in the subtropics and ascent at higher latitudes. Figure 1b shows the standard deviation of the interannual variability. The strong variations occur in the tropical troposphere, collocated with the southern Hadley cell. The linear trend during the 32-yr period is shown in Fig. 1c. The southern Hadley cell is strengthened at the pace of 0–3 ($\times 10^{10}\,\mathrm{kg\,s^{-1}}$) per decade and its northern boundary extends northward. The southern Ferrel cell is also strengthened but with a much weaker magnitude.

The EOF analysis was applied to the streamfunction field between 60°S and 60°N from 1000 to 100 hPa to extract the dominant modes of the interannual variability. To ensure the physical robustness of the EOF analysis (Lian and Chen 2012), the linear trend was removed from the streamfunction field at every grid point before applying the EOF analysis. As shown in Fig. 2a, the strong variability of the streamfunction in the tropics is well captured by the first EOF mode (M1), which explains 46% of the total variance. M1 is similar to the asymmetric mode, or the ''solsticial pattern'' (Lindzen and Hou 1988; Dima and Wallace 2003). It is mainly related to the variability of the southern Hadley cell with a strong cell centered slightly south of the equator and a weaker cell of opposite sign near 30°N, north of the climatological center of the northern Hadley cell.

To better illustrate the variability of the Hadley circulation associated with M1, we constructed the streamfunction composites using six strongest positive years (1979, 1988, 1995, 1996, 1999, and 2010) and the six strongest negative years (1983, 1986, 1994, 1997, 2002, and 2009) according to the time series of M1. As shown in Figs. 2c and 2d, the positive (negative) phase of M1 is featured by a stronger (weaker) southern Hadley cell that is more (less) extensive in the Southern Hemisphere. The ITCZ is centered at about the same latitude (between 5° and 10°N) in both phases but the upward motion is stronger (weaker) and more (less) extensive in the positive (negative) phase of M1. The northern Hadley cell remains weak in both composites, but a close look reveals that the streamfunction gradient, and thus the subsidence, is reduced north of the ITCZ during the positive phase of M1. Figure 2 suggests that the interannual variability of the Hadley circulation is dominated by the intensity change of the ITCZ. Although the ITCZ is located north of the equator, its variability is mainly related to variations of the southern Hadley cell.

Besides NNR2, other datasets including the European Centre for Medium-Range Weather Forecasts Interim Reanalysis (ERA-Interim; Dee et al. 2011) and the NCEP Climate Forecast System Reanalysis (CFSR; Saha et al. 2010) were used to examine the robustness of the streamfunction analysis. An intensifying trend of the southern Hadley cell was found in all datasets, albeit with quantitative differences in the spatial pattern and magnitude of the trend. Although the higher order EOF modes seem more sensitive to the datasets, the first modes in different datasets share the similar dipole pattern, representing the intensity variations of the ITCZ and explaining 45%–56% of the total variance. The correlation coefficients between the principal component time series range from 0.89 to 0.94. The robustness

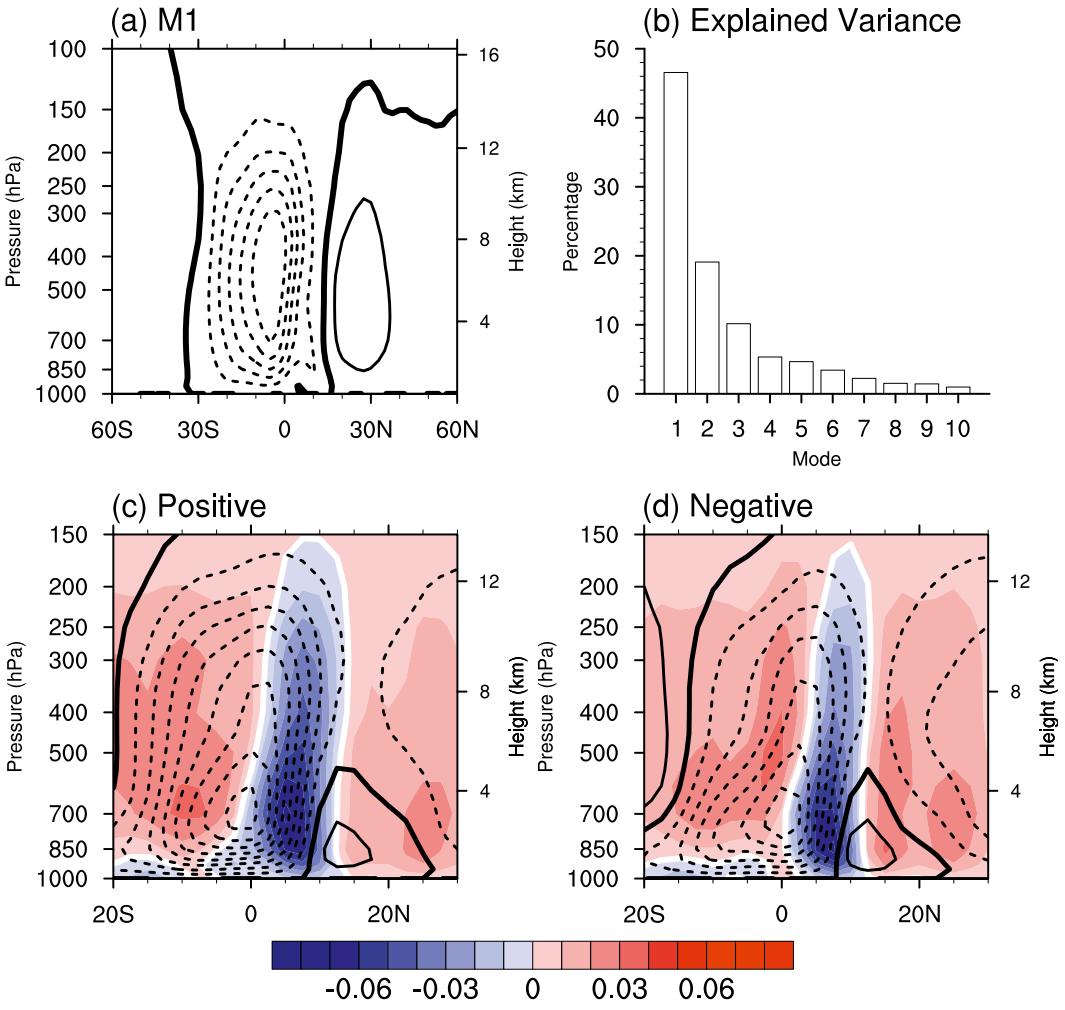

FIG. 2. EOF analysis of the meridional streamfunction in JAS: (a) The leading mode (M1), (b) variance explained by the first 10 modes, and the streamfunction composites (10^{11} kg s^{-1}) for the (c) positive and (d) negative phases of M1. Zero lines are thickened in (a), (c), and (d); solid (dashed) lines indicate positive (negative) values. Contour intervals are 0.02 in (a) and 0.3 × 10^{11} kg s^{-1} in (c) and (d). In (c) and (d) reanalysis ω (Pa s^{-1}) fields are contoured with color and the zero line highlighted in white.

of the EOF analysis was also tested by varying the longitude range over which the streamfunction was averaged, and M1 remains robust when the zonal domain is reduced from 20°–70°W to 20°–50°W. Using the twentieth-century reanalysis dataset (Compo et al. 2011), we found that M1 is a dominant and robust mode for 1871–2010 as well. We will thus focus on this mode in the following sections.

b. *Associations with regional climate factors*

The composite difference of precipitation between the positive and negative phases of M1 (positive minus negative) is shown in Fig. 3. A basinwide precipitation increase occurs over the Atlantic between 0° and 30°N in the positive phase. In particular, precipitation is enhanced significantly along 7°N over the Guiana Highlands, the east Atlantic ITCZ, and between 15° and 20°N over the west Atlantic and Caribbean Sea. The former two changes confirm that M1 is associated with the intensity change, rather than meridional displacement, of the oceanic ITCZ; and the latter is likely associated with the enhanced tropical easterly wave and TC activity. The lack of meridional displacement is likely associated with the dynamic constraints by the low-level convergence of moist energy (Waliser and Somerville 1994), which prevents the ITCZ from migrating farther north in boreal summer. Precipitation also increases over Central America and northern South America. In contrast, the precipitation in the eastern Pacific ITCZ is greatly reduced, which is related to the ENSO pattern over the Pacific.

To examine what SST forcing is related to M1, the composite difference of SST is shown in Fig. 4. The most prominent signature is the SST cooling over the east and

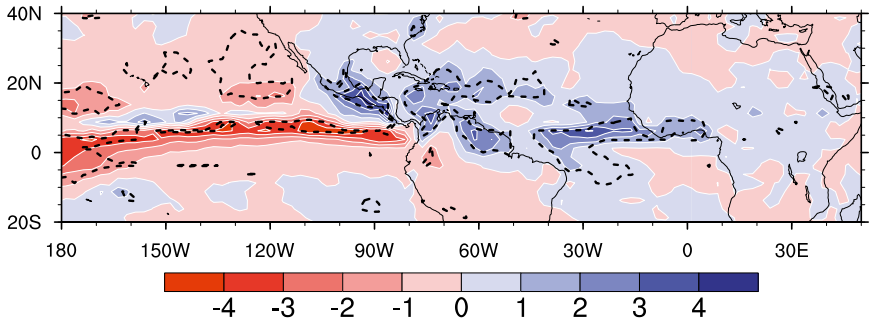

FIG. 3. Composite difference of precipitation based on M1 (mm day^{-1}). Dashed black line indicates the precipitation differences passing the Student's t 95% confidence level.

central Pacific, or the La Niña–like pattern, with the maximum SST difference over the east Pacific up to 1.8 K. Significant warming is found over the tropical western North Atlantic, around the Azores, and in the equatorial Atlantic. Overall the SST anomalies over the Atlantic are reminiscent of a mix of the Atlantic tripole mode (Deser and Timlin 1997) and the Atlantic equatorial mode. The tropical Atlantic warming relative to the subtropics is consistent with the enhanced overturning Hadley circulation in the positive phase of M1.

Interestingly, the basinwide SST pattern in the Atlantic resembles the Pacific pattern but with the opposite polarity. The SST anomaly (SSTA) contrast between the equatorial east Pacific and the equatorial Atlantic leads to an anomalous Walker circulation between the two basins (Fig. 5). The associated low-level westerly anomalies and upper-level easterly anomalies between 130° and 30°W reduce the vertical shear of zonal wind over the equatorial Atlantic. The anomalous Walker circulation is related to the variability of the Atlantic Hadley circulation (Chiang et al. 2002) and contributes to the intensity change of the Atlantic ITCZ. The negative SSTA over the east Pacific also induces significant cooling in the upper troposphere over the east Pacific. The linkage between the Walker circulation and the Hadley circulation provides a teleconnection mechanism for the ENSO to impact the large-scale circulation over the Atlantic. It is also worth pointing out that, although the variations of the Walker circulation are reminiscent of the Madden–Julian oscillation, which modulates Atlantic TC activity on intraseasonal time scales (e.g., Maloney and Hartmann 2000), correlation analysis (not shown) suggests that the MJO, with the ENSO signature removed, is not strongly correlated with M1.

The lag correlations of 3-month mean time series were carried out to identify the relations between M1 and

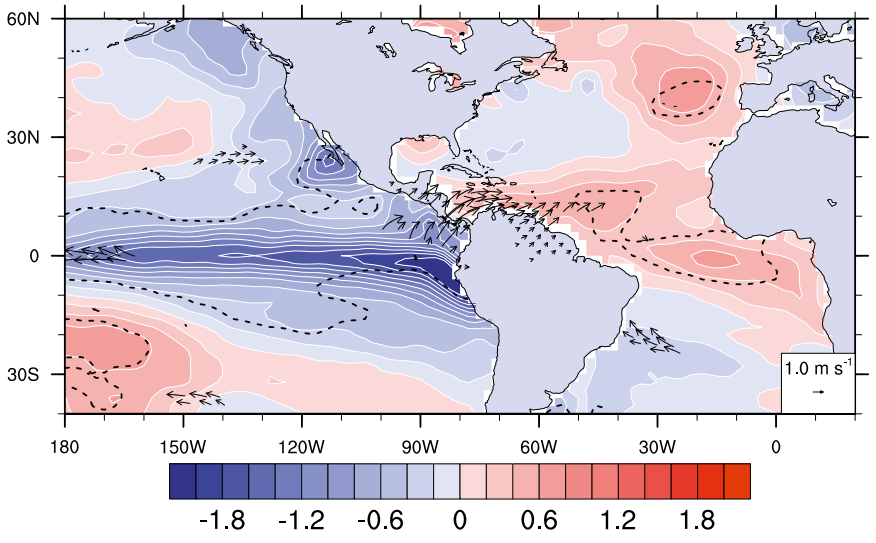

FIG. 4. Composite difference of SST (color) and 10-m wind vector based on M1. Dashed black contours indicate the SST signals passing Student's t 95% confidence level. Only the wind vectors with significant speed changes are plotted.

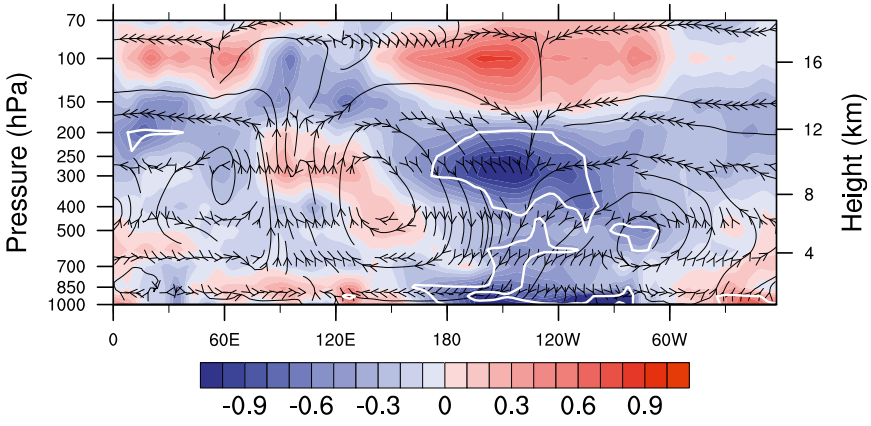

FIG. 5. Zonal cross-section of composite difference based on M1. Air temperature (color, K) and reanalysis wind streamlines are the average between 5°S and 5°N. The white line indicates that the air temperature signal passes the Student's *t* 95% confidence level.

some climate factors in previous seasons (Table 1). All of the time series were first detrended to be consistent with the EOF analysis. The lag correlation between Niño-3.4 and M1 exceeds the 99% confidence level when Niño-3.4 leads M1 by one to three months, and the correlation is strongest (−0.66) when Niño-3.4 leads M1 by 1 month. The lag correlation of the Atlantic meridional mode (AMM) with the leading mode (M1) is above the 95% confidence level from February–April (FMA) (i.e., AMM leading M1 by 5 months) to JJA, and the coefficient increases with decreasing lead time. Weaker but significant correlations were also found between M1 and the AEM index from March–May (MAM) AEM leading M1 by 4 months) to JAS.

Despite the nearly zero simultaneous correlation between the NAO and M1, significant correlations were found between M1 and the NAO in FMA and MAM. The lead correlation between the NAO in MAM and M1 is −0.47 but drops substantially in AMJ. The strong correlations between M1 and the NAO in the previous spring can be interpreted based on some previous studies. The linkage between the NAO and tropical Atlantic SSTA has been long noted (e.g., Marshall et al. 2001). The negative phase of NAO usually leads to the warming over the tropical North Atlantic (TNA) in spring via the weakened trade wind and associated air–sea interaction (Hurrell and Dickson, 2005). The TNA warming may persist into summer and induce the M1 pattern. The SSTA in the extratropical Atlantic (Fig. 4) is also a footprint of the NAO.

In summary, the dominant mode of the interannual variability of the Hadley circulation is associated with the intensity variations of the ITCZ and is also correlated to multiple climate factors. All of these factors—ENSO, NAO, and AMM—are known to impact Atlantic TC activity (Kossin and Vimont 2007; Kozar et al. 2012). In the next section, we will investigate the impacts of M1 on Atlantic TC activity.

4. Impacts of the Hadley circulation variability on Atlantic TCs

To examine the impacts of M1 on the Atlantic TC activity, we constructed storm track composites for the positive and negative phases of M1 (Fig. 6). The colors along the tracks indicate the storm intensity. The most striking difference is that a larger number of TCs developed in the positive phase composite: there are 59 storms in the six positive-phase composite years and 34 storms in the six negative-phase composite years, while the average storm number in JAS during 1979–2010 is about 8.3. Comparison of the composites further reveals a substantial increase in the number of TCs forming over the MDR in the positive phase. Developing over the open ocean, these storms have a longer time traveling over the warm ocean and thus a greater chance to develop into a major hurricane (Vimont and Kossin 2007; Kossin and Vimont 2007). Among the 59 TCs, there are 35 (~59%) hurricanes and 22 (~37%) major hurricanes

TABLE 1. Lag correlation between M1 (JAS) and detrended climate indices. Values in italic and parentheses are above the 95% confidence level, and those in italic bold exceed the 99% confidence level.

	JFM	FMA	MAM	AMJ	MJJ	JJA	JAS
Niño 3.4	−0.01	−0.08	−0.24	***−0.46***	***−0.62***	***−0.66***	***−0.65***
AMM	0.34	(*0.36*)	(*0.39*)	***0.45***	***0.49***	***0.49***	***0.53***
AEM	0.27	0.30	(*0.35*)	(*0.41*)	(*0.44*)	***0.47***	***0.47***
NAO	−0.25	(*-0.37*)	***−0.47***	−0.27	−0.11	0.05	−0.02

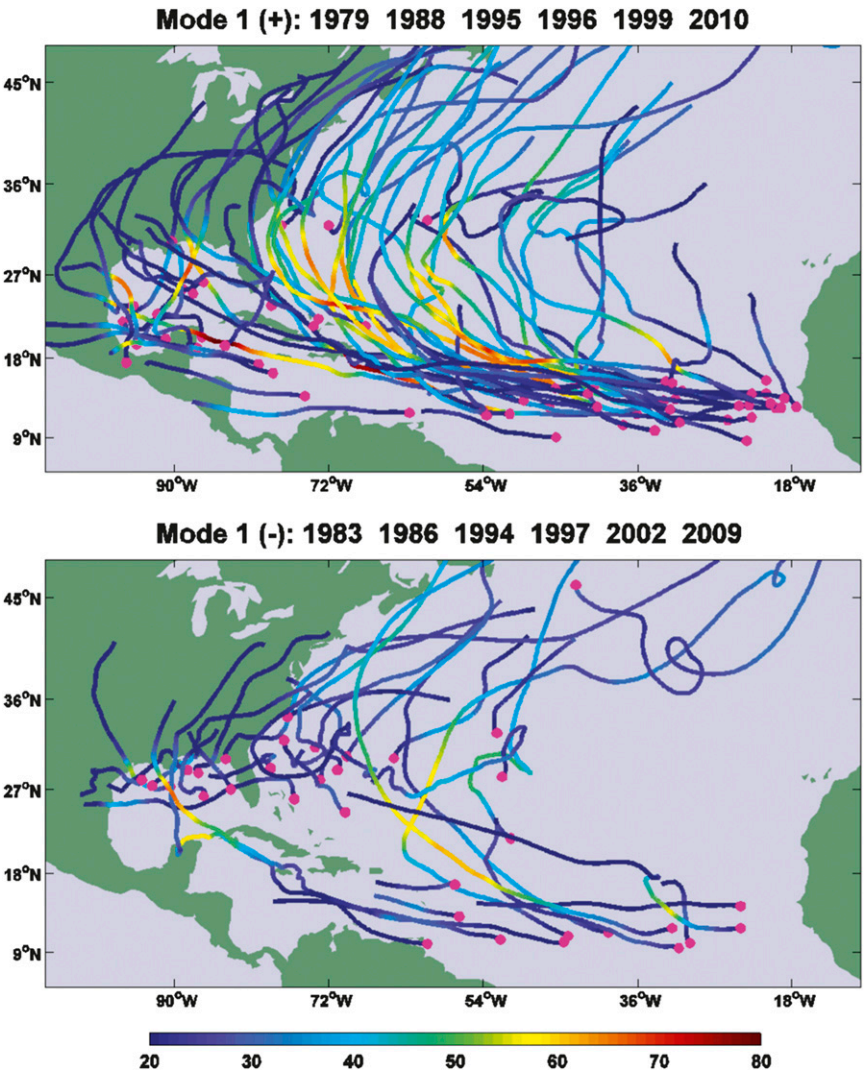

FIG. 6. Storm track, intensity, and genesis location in JAS for the positive and negative phases of M1. Genesis locations are indicated by the pink dots, and the storm intensity in terms of the maximum surface wind speed ($m\,s^{-1}$) is indicated by colors of storm tracks. The composite years for each phase are listed at the top of each plot.

(Category 3 or above). In the negative phase of M1, TC genesis shifts northwestward, and there is a larger fraction of TCs forming near the southeast U.S. coast. These storms had short tracks before making landfall or curving northward. Even some of the MDR storms also had very short tracks, and only two MDR TCs tracked across the Caribbean Sea, leaving the ocean south of the Greater Antilles free of TCs. Among the 34 storms, there are only 15 (~44%) hurricanes and 6 (~18%) major hurricanes, in sharp contrast to the positive phase composite.

The composites of M1 suggest that variations of the Atlantic TC activity (JAS) are closely related to the variations of the Hadley circulation. In the following discussion, we will investigate how M1 affects the Atlantic TC activity.

a. The large-scale environment

The SST composite difference in Fig. 4 implies a more favorable thermodynamic environment for Atlantic TC activity during the positive phase of M1. The increase of SST in the tropical North Atlantic indicates greater ocean heat content, the impacts of which on TCs have long been recognized (e.g., Gray 1968). The cold SST anomalies over the east Pacific contribute to a lower tropical mean SST and thus higher relative SST (defined as the difference between the local SST and the tropical mean SST) over the tropical North Atlantic. The relative

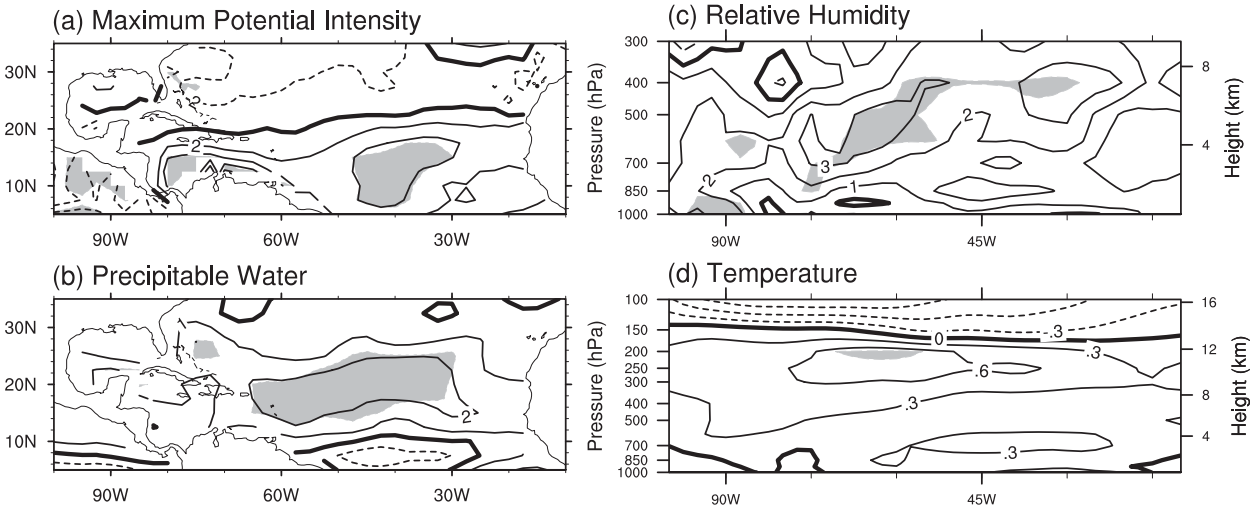

FIG. 7. Composite differences of (a) maximum potential intensity, (b) total precipitable water, (c) relative humidity (10°–30°N average), and (d) temperature (10°–30°N average). Contour intervals are 2 m s^{-1}, 1.0 mm, 1%, and 0.3 K in (a)–(d). Zero lines are thickened, and solid (dashed) lines indicate positive (negative) values. Solid shading indicates differences above the 95% confidence level. In (a) and (b) values over land are masked.

SST can serve as a proxy of TC maximum potential intensity (Vecchi and Soden 2007) and is closely related to Atlantic tropical cyclone activity (e.g., Swanson 2008; Vecchi et al. 2008). The composite difference of the relative SST (not shown) is very similar to that of the absolute SST (Fig. 4) over the Atlantic except that the significant warming extends west of 30°W to the entire main development region.

Consistent with the changes in SST, the TC potential intensity (Emanuel 1995) increases over the central Atlantic (Fig. 7a). Aside from SST, the TC maximum potential intensity also depends on temperature and moisture profiles of the atmosphere. Figure 7b shows that the total precipitable water increases significantly over the tropical North Atlantic between 12° and 25°N. Total precipitable water (or column water vapor) has a strong control on precipitation and tropical cyclone formation (Raymond 2000; Bretherton et al. 2004; Neelin et al. 2009), and a deep moist layer is favorable for the onset of deep convection. The vertical cross section of relative humidity (Fig. 7c) shows that significant changes mostly occur in the middle troposphere between 400 and 700 hPa. Different from the more vertically extensive distribution of cold temperature anomalies over the equatorial region (Fig. 5), the upper-level cooling associated with the ENSO component is mostly confined above 150 hPa and is not statistically significant (Fig. 7d). The vertical cross section of air temperature implies that M1 is not associated with significant variations of troposphere static stability over the MDR.

As mentioned in the previous sections, M1 is associated with prominent changes of the large-scale overturning circulations in which the variations of the upper-level and lower-level flows may lead to significant changes in vertical wind shear. Figure 8a shows that VWS is reduced during the positive phase of M1 over most of the MDR, the Gulf of Mexico, and especially over the Caribbean Sea, where the VWS difference is as large as 8 m s^{-1}. Differences of VWS with a similar pattern and a smaller magnitude are also found in the lower troposphere (between 500 and 850 hPa, Fig. 8b). Strong VWS is known to be detrimental for TC formation and intensification (e.g.,

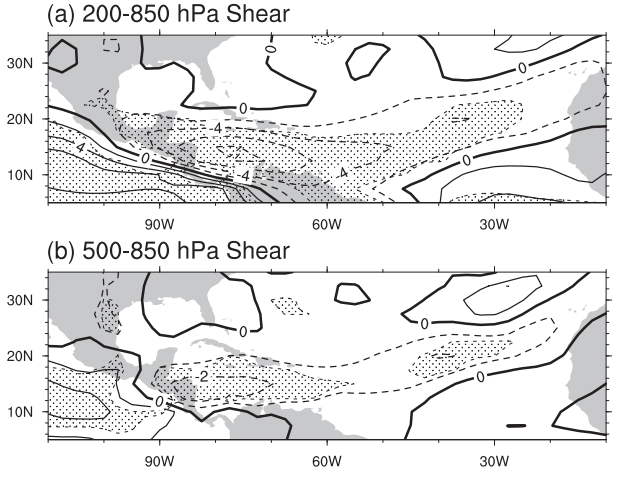

FIG. 8. Composite differences of the (a) 200–850-hPa and (b) 500–850-hPa vertical wind shear (vector wind difference): contour intervals are 2.0 m s^{-1} and 1.0 m s^{-1}, respectively; Zero lines are thickened, and solid (dashed) lines indicate positive (negative) values. Shading indicates differences above the 95% confidence level.

Gray 1968; DeMaria 1996), and reduced (enhanced) VWS in the positive (negative) phase of M1 contributes to a more (less) active hurricane season over the Atlantic.

The impacts of the subtropical high on Atlantic TC tracks have been noted by many previous studies (e.g., Kossin et al. 2010; Colbert and Soden 2012). The subtropical high is closely related to subtropical subsidence of the Hadley circulation. The streamfunction in Figs. 2c and 2d shows weakened (enhanced) subtropical subsidence north of 20°N in the positive (negative) phase of M1, implying a weaker (stronger) subtropical high. Figures 9a and 9b confirm this and further show that the subtropical high retreats eastward in the positive phase of M1. The associated changes in the steering flow allow tropical cyclones to recurve northeastward over the central Atlantic (Fig. 6). Consequently, the number of landfalling TCs does not increase proportionally with the total TC number in JAS. Figure 9c reveals a significant decrease in the 850-hPa geopotential height over the tropical and subtropical North Atlantic, especially over the Gulf of Mexico and the west Atlantic, in the positive phase of M1. A similar drop is also found in sea level pressure (not shown). This is consistent with the inverse relationship between sea level pressure and Atlantic tropical cyclone activity reported in previous studies (e.g., Shapiro 1982; Gray 1984b) and confirms the link between reduced subsidence and pressure decrease suggested by Knaff (1997).

We also examined the changes of the low-level divergence and vorticity associated with M1 (not shown). During the positive phase of M1 (i.e., when the ITCZ is stronger), positive vorticity anomalies and enhanced convergence were found in the lower troposphere over the MDR, consistent with the TC activity increase.

In summary, various aspects of the large-scale conditions are favorable for TC formation and intensification in the positive phase of M1. However, the large-scale conditions alone cannot explain the enhanced TC activity over the east Atlantic. The composite differences of the thermodynamic variables, such as absolute (relative) MDR SST (Fig. 4) and the TC potential intensity (Fig. 7a), are relatively weak and statistically insignificant over the east Atlantic. Furthermore, the 200–850-hPa VWS even increases slightly in this region (Fig. 8). In fact, even if the large-scale environment is both thermodynamically and dynamically favorable, a finite-amplitude cyclonic precursor disturbance is still a necessary condition for tropical cyclogenesis on a realistic time scale (e.g., Nolan et al. 2007). Over the Atlantic a majority of the tropical cyclones originated from tropical easterly waves. In the next subsection we will examine the hypothesis that the variability of the Hadley circulation can impact the Atlantic TC activity indirectly via modulating the frequency and structure of TEWs.

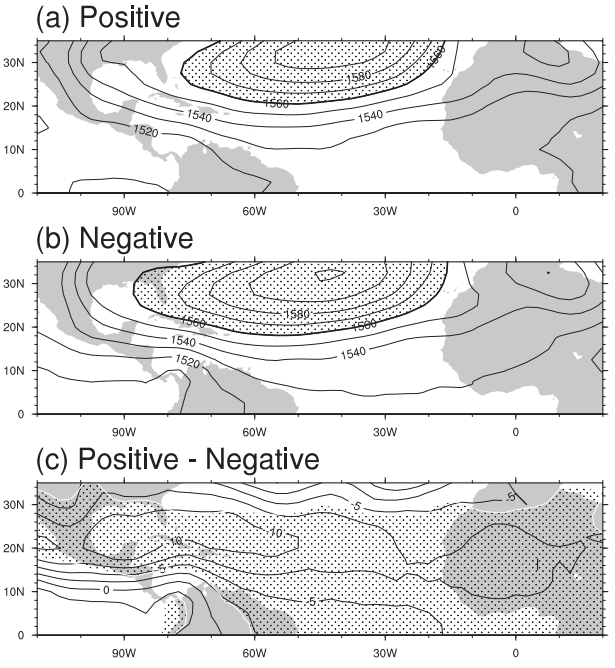

FIG. 9. Composite means of 850-hPa geopotential height (gpm) for the (a) positive and (b) negative phases of M1, and (c) the composite difference of 850-hPa geopotential height. Geopotential height greater than 1560 gpm is highlighted with stippling in (a) and (b). The stippling in (c) indicates the composite differences exceeding the 95% confidence level.

b. *Tropical easterly waves*

One of the necessary conditions for TC formation in the present climate is a preexisting low-level cyclonic disturbance. To examine the variations of TEW activity, we calculated the eddy kinetic energy (EKE) of the 2.5- to 9-day bandpass filtered 850-hPa wind and constructed composites based on the positive and negative phases of M1. Figure 10a shows the positive composite. A strong wave center was found at the west coast of Africa, around 12°N, where AEWs usually intensify through interaction with mesoscale convective systems (Berry and Thorncroft 2005; Ventrice et al. 2012). The strong wave activity can be tracked east of the prime meridian, and a second track along 20°N is also discernible, which is related to eastward propagating disturbances north of the African easterly jet (Pytharoulis and Thorncroft 1999). The wave activity extends westward to the ocean but weakens away from the coast. The strong variances over the subtropical western North Atlantic can be attributed to TEWs, midlatitude disturbances, and TCs.

Figures 10b and 10c show the composite of wave activity in the negative phase of M1 and the composite difference between the positive and negative phases, respectively. Compared to the positive phase, the wave activity is reduced over West Africa, along the wave track over the

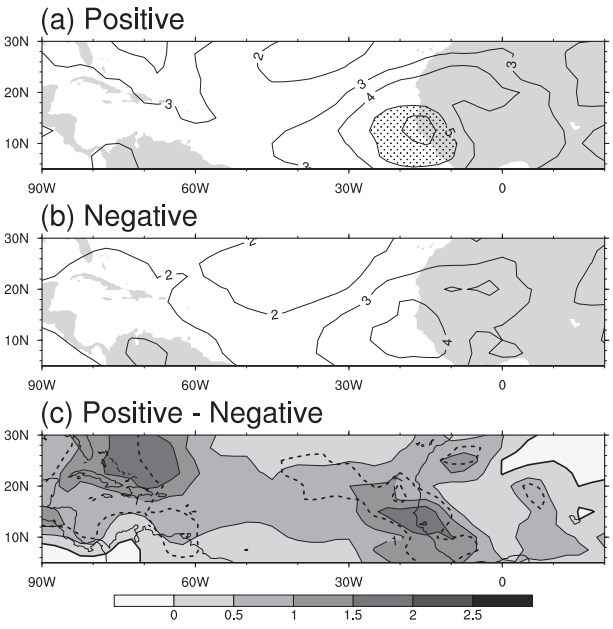

FIG. 10. Eddy kinetic energy ($m^2 s^{-2}$) of 2.5- to 9-day bandpass filtered wind (850 hPa): the composite means for the (a) positive and (b) negative phases of M1, and (c) the composite difference. Values greater than $5 m^2 s^{-2}$ are shaded; the dashed black line in (c) indicates that the signal passes the Student's t 95% confidence level.

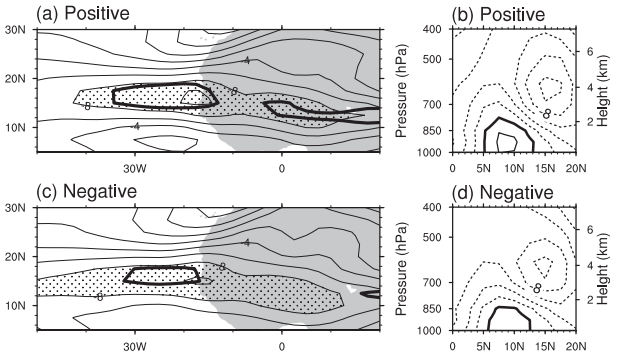

FIG. 11. Composites of zonal wind for the (a),(b) positive and (c),(d) negative phases of M1. In (a) and (c) the 700-hPa zonal wind is plotted with thin contours (values less than $-8.0 m s^{-1}$ are stippled); thick black contour outlines the region where the meridional gradient of absolute vorticity (i.e., beta-U_{yy}) is negative. In (b) and (d) the cross section of zonal wind (15°–30°W average) is plotted: contour interval $2 m s^{-1}$. Zero lines are thickened, and solid (dashed) lines indicate positive (negative) values.

MDR, the Caribbean Sea, and the Gulf of Mexico. Enhanced wave activity in the positive phase of M1 was also found at 700 hPa, especially near the West African coast. The large variances can be attributed to stronger waves and/or more frequent occurrence of waves. The increases in wave intensity (e.g., Arnault and Roux 2011) and frequency (e.g., Thorncroft and Hodges 2001) have been suggested as favorable for TC formation over the Atlantic.

Most TEWs found near the African coast originate in West Africa. African easterly waves can be regarded as perturbations excited by finite-amplitude, transient heating in a linearly stable mean state (Thorncroft et al. 2008). The mean flow may not be unstable enough to maintain or amplify the waves, but the idealized simulation by Leroux and Hall (2009) showed that the wave response is very sensitive to the structure of the mean flow. Strong waves are associated with a strong jet that has a strong vertical shear in the lower troposphere or a strong and extended potential vorticity reversal. The composites of the 700-hPa seasonal mean (JAS) zonal flow are shown in Fig. 11. Over West Africa and the east Atlantic, although the easterly jet has a similar maximum intensity in both composites, the jet in the positive composite is characterized by a stronger cyclonic shear south of the jet core and a larger area of absolute vorticity gradient reversal. The enhanced cyclonic shear is mainly contributed by the weaker easterly flow south of 12°N. The extended area of absolute vorticity gradient reversal implies a stronger instability and thus a better chance for wave growth. Figure 11 also shows that the easterly jet weakens more sharply over the Atlantic as extending westward from the West African coast in the positive phase of M1, which implies stronger wave accumulation at the jet exit region (Webster and Chang 1988; Done et al. 2011). The vertical cross sections of the zonal wind show that the low-level westerly flow is enhanced in the positive phase of M1 (Figs. 11b,d). The stronger monsoonal westerly flow is consistent with the stronger ITCZ. The flow increases the near-coast moisture convergence and low-level vertical shear, favoring the coastal development of AEWs. The enhanced inland moisture transport may also contribute to the positive precipitation anomalies over West Africa, shown in Fig. 3 (Pu and Cook 2012). In summary, variations of the TEW activity can be attributed to changes of the mean flow and changes of convective activity near the coast of West Africa.

Besides the wave frequency and intensity (Thorncroft and Hodges 2001; Camara et al. 2011), another aspect of the TEWs that affects their subsequent evolution is the wave structure (Hopsch et al. 2010), in particular, the existence and vertical structure of the wave pouch (Dunkerton et al. 2009). Wang et al. (2012) suggested that a deep pouch extending from the middle troposphere (~600 hPa) to the boundary layer is a necessary (but not sufficient) condition for TC formation within an easterly wave. Next we will examine the wave pouch frequency and vertical coherence for the positive and negative phases of M1.

A wave pouch is a region of cyclonic rotation and weak deformation. We use the following two criteria to estimate the wave pouch frequency: 1) OW $> 1.0 \times 10^{-10}\,\mathrm{s}^{-2}$ and 2) $\zeta > 1.0 \times 10^{-6}\,\mathrm{s}^{-1}$, where ζ is the relative vorticity and the Okubo–Weiss parameter is defined as

$$\mathrm{OW} \equiv \xi^2 - s_n^2 - s_s^2 \tag{7}$$

in which s_n and s_s are the normal and shear components of flow strain[1] (Rozoff et al. 2006). The positive values of OW indicate that the flow is rotation dominant. The 2.5-day low-pass filtered data were used to calculate the pouch frequency as the background flow needs to be taken into account for the formation of a wave pouch. Note that the threshold of OW used here is relatively small. This is to include weak wave pouches that may not develop into TCs. To avoid contamination by TCs, all grid points within a 12.5° diameter from a TC along 6-hourly HURDAT storm tracks were excluded. The criteria work reasonably well when compared with the operational pouch tracking products (Montgomery et al. 2012).

The composite of 850-hPa wave pouch frequency in the positive phase of M1 is shown in Fig. 12a. The nonzero pouch frequency region follows the wave track, which is south of the jet over North Africa and extends westward and slightly northward to the southeast U.S. coast. High frequency of occurrence is found along the northern and southern wave tracks over West Africa and along the wave track over the east Atlantic, with a maximum off the coast of West Africa. The center of high frequency near Panama is caused by shallow stationary vortices, which are typically irrelevant to Atlantic TC activity in JAS. Cyclogenesis locations, especially for the MDR storms, largely fall into the regions of high pouch frequency. Figures 11b and 11c show significant reductions of the pouch frequency over West Africa, the Atlantic MDR, and the Caribbean Sea in the negative phase of M1, which is consistent with the reduced TC activity.

To examine the vertical structure of wave pouches, we examine the frequency of occurrence of ''deep'' wave pouches in the lower troposphere. The vorticity and OW were examined at 500-, 600-, 700-, and 850-hPa levels over each grid point, and a wave pouch is designated as a deep pouch if at least three out of four levels satisfy the aforementioned criteria. This is to exclude shallow or strongly tilted wave pouches. As shown in Fig. 13a, high frequency of deep pouches of 10–14 days per season

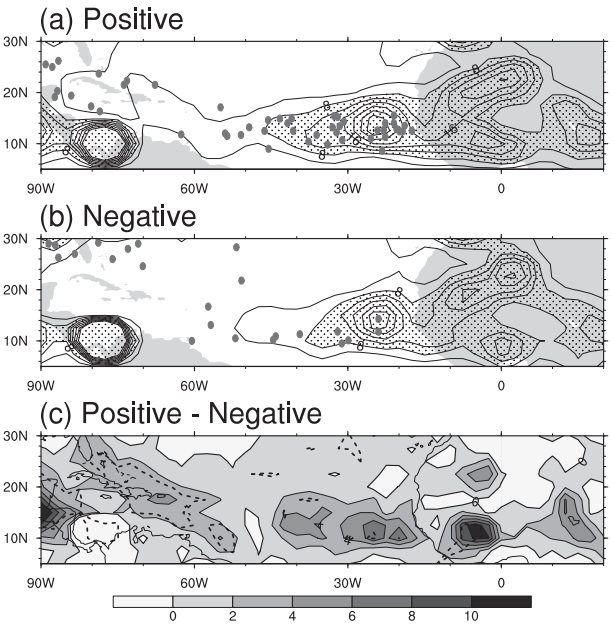

FIG. 12. Wave pouch frequency (850 hPa; unit is days per season) for (a) the positive phase, (b) the negative phase, and (c) the composite difference. The contour interval is 4 days per season in (a) and (b), and the contoured range is [0, 32]; values greater than eight days per season are stippled. The black dots are the TC genesis locations in corresponding seasons. The dashed black line in (c) indicates the signal passes the 95% confidence level.

occurs along 10°–12°N over West Africa and the east Atlantic in the positive phase of M1, consistent with the more frequent TC genesis in the east Atlantic. The northern wave track over West Africa is still discernible but has a much lower frequency than the southern one. This is consistent with previous findings that the northern waves generally have a shallow structure confined to 850 hPa and below (e.g., Pytharoulis and Thorncroft 1999). The composite based on the negative phase of M1 (Fig. 13b) has a similar spatial pattern, but the frequency of deep pouches is significantly reduced along the wave track over West Africa and the east Atlantic, over the Caribbean Sea, and over Central America (Fig. 13c).

The above diagnoses suggest that M1 affects TC activity indirectly via modulating the wave pouch frequency and structure, especially over the east Atlantic and the Caribbean Sea. When the ITCZ is stronger (the positive phase of M1), more waves develop a favorable pouch structure for TC formation. It should be emphasized that the variations of the TEWs are not independent of the variations of the large-scale circulation. For example, the warm SST and a moist troposphere associated with the stronger ITCZ (the positive phase of M1) and the anomalous Walker circulation are all conducive to convective development, which is believed to play an

[1] Okubo–Weiss parameter components: $\xi = \frac{\partial v}{\partial x} - \frac{\partial u}{\partial y}$, $s_n = \frac{\partial u}{\partial x} - \frac{\partial v}{\partial y}$, $s_s = \frac{\partial v}{\partial x} + \frac{\partial u}{\partial y}$

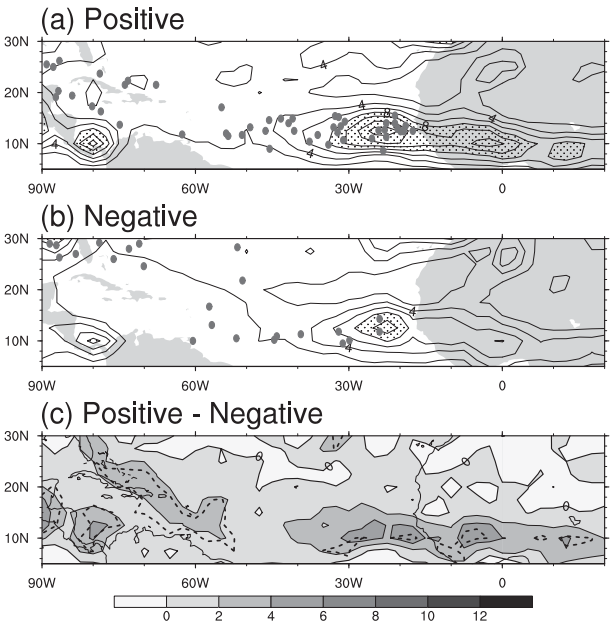

FIG. 13. As in Fig. 12 but for the frequency of vertically coherent wave pouches: the contour interval is two days per season in (a) and (b), and the contoured range is [0, 16].

important role in the maintenance and intensification of TEWs (e.g., Berry and Thorncroft 2005; Thorncroft et al. 2008). Besides, a wave pouch is more likely to develop a vertically coherent structure if vertical wind shear (VWS) is weak (Wang et al. 2012; Raymond and López Carrillo 2011; Davis and Ahijevych 2012).

c. *On the seasonal transition in October*

The Atlantic Hadley circulation mean state changes significantly in October (the southern cell dwindles while the northern cell strengthens), which is accompanied by the variations of the monthly mean VWS across the basin. October also marks a significant change of the atmospheric sounding profile and the air mass source over the tropical North Atlantic and the Caribbean (Dunion 2011). Correspondingly, the TC genesis over the east Atlantic diminishes, but more storms develop over the west Atlantic and Caribbean and are increasingly affected by midlatitude fronts (http://www.nhc.noaa.gov/climo/).

Nevertheless, the interannual variability of the Hadley circulation in October is still dominated by a dipole pattern similar to M1, and the leading EOF mode of the June–October (JASO) seasonal mean meridional streamfunction resembles that of the JAS seasonal mean (i.e., M1; figures not shown). The time series of the two leading EOF modes have a correlation coefficient of ~0.96 during 1979–2010, and both time series are significantly correlated with the detrended Atlantic hurricane number, accumulated cyclone energy, Niño-3.4, Atlantic meridional mode, absolute and relative MDR SST, Sahel precipitation index (Janowiak 1988), and some large-scale environmental parameters over the Atlantic (Table 2). The same table also shows that the correlations with the Atlantic multidecadal oscillation (AMO) (Enfield et al. 2001) are below the 95% confidence level. Moreover, easterly wave activity is enhanced over the Caribbean in October in the positive phase of M1, consistent with the local TC genesis increase (not shown). These results further confirm the robustness of M1 and its impacts on Atlantic TC activity.

5. Summary and discussion

The interannual variability of the Hadley circulation in boreal summer and its impacts on the Atlantic TC activity were examined in this study. A novel method was developed to define the regional Hadley circulation in terms of a meridional streamfunction derived from the irrotational component of the meridional flow. The long-term mean summer seasonal streamfunction over the Atlantic consists of a prominent southern Hadley cell and a dwarfed northern Hadley cell, which is similar to the solsticial pattern in the global streamfunction average (Lindzen and Hou 1988; Dima and Wallace 2003).

The EOF analysis was employed to study the interannual variability of the Hadley circulation over the Atlantic. The leading mode explains more than 45% of the total variance and is mainly associated with the variations of the southern Hadley cell and the intensity change of the ITCZ. This leading mode (M1) is significantly correlated to different climate factors, including the ENSO, AMM, NAO, and the absolute/relative SST

TABLE 2. Correlations between leading mode (M1) and detrended climate indices (JAS and JASO): the detrended Atlantic hurricane number (Hurr num), accumulated cyclone energy (ACE), the shear between 200-hPa and 850-hPa wind vectors (VWS), the 850-hPa relative vorticity (VOR) and relative humidity (RH), and the mean sea level pressure (MSLP), as well as the correlations with the Atlantic multidecadal oscillation (AMO), are all averaged over the MDR. Values in italic and brackets are above the 95% confidence level, and those in italic bold exceed the 99% confidence level.

	Hurr Num	ACE	Niño-3.4	AMM	AMO	Sahel rain	MDR SST	Rel SST	VWS	VOR	RH	MSLP
M1 (JAS)	***0.66***	***0.69***	***−0.65***	***0.53***	0.34	***0.47***	***0.46***	***0.66***	***−0.75***	***0.63***	(*0.44*)	***−0.67***
M1 (JASO)	***0.72***	***0.71***	***−0.62***	***0.48***	0.32	(*0.43*)	(*0.38*)	***0.62***	***−0.76***	***0.63***	***0.50***	***−0.64***

over the tropical North Atlantic. The Atlantic TC activity is strongly impacted by M1. In the positive phase of M1 (when the ITCZ is stronger than normal), there are more TCs forming over the main development region with a larger fraction intensifying into major hurricanes. In the negative phase of M1, the Atlantic TC genesis frequency is lower than normal, and the genesis locations shift northwestward to the Gulf of Mexico and the western North Atlantic. The positive phase of M1 is characterized by weaker vertical wind shear, higher tropospheric water vapor content, stronger low-level convergence and vorticity, as well as more propitious tropical easterly wave activity, all of which are favorable for the TC formation and intensification. M1 thus unifies both dynamic and thermodynamic conditions impacting Atlantic TC activity.

The role of TEWs in modulating the Atlantic TC activity is highlighted in this study. In the positive phase of M1, the wave activity (in terms of EKE of bandpass filtered data) is significantly enhanced over the east Atlantic and Caribbean Sea, which can be attributed to the changes of the mean flow and stronger coastal convection. In the context of the recently proposed marsupial paradigm (Dunkerton et al. 2009), we also examined the frequency and structure of the wave pouches associated with different phases of M1. The vertically coherent pouch structure of TEWs was suggested as a necessary and highly favorable condition for TC formation (Wang et al. 2012). In the positive phase of M1, wave pouches occur more frequently at 850 hPa over the MDR, and the number of wave pouches with a vertically coherent structure also increases significantly. Our study thus suggests that the variability of the Hadley circulation impacts the Atlantic TC activity by modulating the large-scale conditions as well as the frequency and structure of TEWs.

The strong correlations between M1 and different climate factors, such as ENSO, AMM, NAO, and the TNA SST, suggest that M1 may be induced by different climate forcings. This implies that different climate forcings may affect Atlantic tropical cyclone activity through the same dynamic and thermodynamic mechanisms by modulating the Hadley circulation. The Hadley circulation thus provides a useful perspective to understand the variability and predictability of TC activity over the Atlantic. Whether a similar dominant mode of the Hadley circulation exists over other basins and whether and how it modulates TC activity in those basins (if it exists) warrants further investigation.

Acknowledgments. The authors thank Dr. Timothy J. Dunkerton for stimulating discussion. The maximum potential intensity calculation routine and the TC track plotting routine were kindly provided by Dr. Kerry A. Emanuel. We also thank three anonymous reviewers for constructive comments. The research data was provided by NOAA/OAR/ESRL PSD. This work is supported by the National Science Foundation Grants ATM-1016095 and ATM-1118429 and the Office of Naval Research Grant N00014-11-1-0446.

REFERENCES

Adler, R. F., and Coauthors, 2003: The version-2 Global Precipitation Climatology Project (GPCP) monthly precipitation analysis (1979–present). *J. Hydrometeor.,* **4,** 1147–1167.

Arnault, J., and F. Roux, 2011: Characteristics of African easterly waves associated with tropical cyclogenesis in the Cape Verde Islands region in July-August-September of 2004–2008. *Atmos. Res.,* **100,** 61–82.

Berry, G. J., and C. Thorncroft, 2005: Case study of an intense African easterly wave. *Mon. Wea. Rev.,* **133,** 752–766.

Bretherton, C. S., M. E. Peters, and L. E. Back, 2004: Relationships between water vapor path and precipitation over the tropical oceans. *J. Climate,* **17,** 1517–1528.

Camara, A., A. Diedhiou, and A. Gaye, 2011: African easterly waves and cyclonic activity over the eastern Atlantic: Composite and case studies. *Int. J. Geophys.,* **2011,** 874292, 14 pp.

Chang, P., R. Saravanan, L. Ji, and G. C. Hegerl, 2000: The effect of local sea surface temperatures on atmospheric circulation over the tropical Atlantic sector. *J. Climate,* **13,** 2195–2216.

Chiang, J. C. H., and D. J. Vimont, 2004: Analogous Pacific and Atlantic meridional modes of tropical atmosphere–ocean variability. *J. Climate,* **17,** 4143–4158.

——, Y. Kushnir, and A. Giannini, 2002: Deconstructing Atlantic intertropical convergence zone variability: Influence of the local cross-equatorial sea surface temperature gradient and remote forcing from the eastern equatorial Pacific. *J. Geophys. Res.,* **107,** 4004, doi:10.1029/2000JD000307.

Colbert, A. J., and B. J. Soden, 2012: Climatological variations in North Atlantic tropical cyclone tracks. *J. Climate,* **25,** 657–673.

Compo, G. P., and Coauthors, 2011: The Twentieth Century Reanalysis Project. *Quart. J. Roy. Meteor. Soc.,* **137,** 1–28.

Davis, C. A., and D. A. Ahijevych, 2012: Mesoscale structural evolution of three tropical weather systems observed during PREDICT. *J. Atmos. Sci.,* **69,** 1284–1305.

Dee, D. P., and Coauthors, 2011: The ERA-Interim reanalysis: Configuration and performance of the data assimilation system. *Quart. J. Roy. Meteor. Soc.,* **137,** 553–597.

DeMaria, M., 1996: The effect of vertical shear on tropical cyclone intensity change. *J. Atmos. Sci.,* **53,** 2076–2088.

Deser, C., and M. S. Timlin, 1997: Atmosphere–ocean interaction on weekly timescales in the North Atlantic and Pacific. *J. Climate,* **10,** 393–408.

Dima, I. M., and J. M. Wallace, 2003: On the seasonality of the Hadley cell. *J. Atmos. Sci.,* **60,** 1522–1527.

Doblas-Reyes, F. J., and M. Déqué, 1998: A flexible bandpass filter design procedure applied to midlatitude intraseasonal variability. *Mon. Wea. Rev.,* **126,** 3326–3335.

Done, J. M., G. J. Holland, and P. Webster, 2011: The role of wave energy accumulation in tropical cyclogenesis over the tropical North Atlantic. *Climate Dyn.,* **36,** 753–767.

Dunion, J. P., 2011: Rewriting the climatology of the tropical North Atlantic and Caribbean Sea atmosphere. *J. Climate,* **24,** 893–908.

Dunkerton, T. J., M. T. Montgomery, and Z. Wang, 2009: Tropical cyclogenesis in a tropical wave critical layer: Easterly waves. *Atmos. Chem. Phys.,* **9,** 5587–5646.

Emanuel, K. A., 1995: Sensitivity of tropical cyclones to surface exchange coefficients and a revised steady-state model incorporating eye dynamics. *J. Atmos. Sci.,* **52,** 3969–3976.

——, 2007: Environmental factors affecting tropical cyclone power dissipation. *J. Climate,* **20,** 5497–5509.

Enfield, D. B., A. M. Mestas-Nunez, and P. J. Trimble, 2001: The Atlantic multidecadal oscillation and its relationship to rainfall and river flows in the continental U.S. *Geophys. Res. Lett.,* **28,** 2077–2080.

Fang, J., and F. Zhang, 2010: Initial development and genesis of Hurricane Dolly (2008). *J. Atmos. Sci.,* **67,** 655–672.

Goldenberg, S. B., C. W. Landsea, A. M. Mestas-Nuñez, and W. M. Gray, 2001: The recent increase in Atlantic hurricane activity: Causes and implications. *Science,* **293,** 474–479.

Gray, W. M., 1968: Global view of the origin of tropical disturbances and storms. *Mon. Wea. Rev.,* **96,** 669–700.

——, 1984a: Atlantic seasonal hurricane frequency. Part I: El Niño and 30-mb quasi-biennial oscillation influences. *Mon. Wea. Rev.,* **112,** 1649–1668.

——, 1984b: Atlantic seasonal hurricane frequency. Part II: Forecasting its variability. *Mon. Wea. Rev.,* **112,** 1669–1683.

——, and C. W. Landsea, 1992: African rainfall as a precursor of hurricane-related destruction on the U.S. East Coast. *Bull. Amer. Meteor. Soc.,* **73,** 1352–1364.

Hack, J. J., W. H. Schubert, D. E. Stevens, and H.-C. Kuo, 1989: Response of the Hadley circulation to convective forcing in the ITCZ. *J. Atmos. Sci.,* **46,** 2957–2973.

Hopsch, S. B., C. D. Thorncroft, K. Hodges, and A. Aiyyer, 2007: West African storm tracks and their relationship to Atlantic tropical cyclones. *J. Climate,* **20,** 2468–2483.

——, ——, and K. R. Tyle, 2010: Analysis of African easterly wave structures and their role in influencing tropical cyclogenesis. *Mon. Wea. Rev.,* **138,** 1399–1419.

Hurrell, J. W., and R. R. Dickson, 2005: Climate variability over the North Atlantic. *Marine Ecosystems and Climate Variation,* N. C. Stenseth et al., Eds., Oxford University Press, 15–31.

Janowiak, J. E., 1988: An investigation of interannual rainfall variability in Africa. *J. Climate,* **1,** 240–255.

Kanamitsu, M., W. Ebisuzaki, J. Woollen, S. Yang, J. J. Hnilo, M. Fiorino, and G. L. Potter, 2002: NCEP-DOE AMIP-II Reanalysis (R-2). *Bull. Amer. Meteor. Soc.,* **83,** 1631–1643.

Knaff, J. A., 1997: Implications of summertime sea level pressure anomalies in the tropical Atlantic region. *J. Climate,* **10,** 789–804.

Kossin, J. P., and D. J. Vimont, 2007: A more general framework for understanding Atlantic hurricane variability and trends. *Bull. Amer. Meteor. Soc.,* **88,** 1767–1781.

——, S. J. Camargo, and M. Sitkowski, 2010: Climate modulation of North Atlantic hurricane tracks. *J. Climate,* **23,** 3057–3076.

Kozar, M. E., M. E. Mann, S. J. Camargo, J. P. Kossin, and J. L. Evans, 2012: Stratified statistical models of North Atlantic basin-wide and regional tropical cyclone counts. *J. Geophys. Res.,* **117,** D18103, doi:10.1029/2011JD017170.

Landsea, C. W., 1993: A climatology of intense (or major) Atlantic hurricanes. *Mon. Wea. Rev.,* **121,** 1703–1713.

——, and W. M. Gray, 1992: The strong association between western Sahelian monsoon rainfall and intense Atlantic hurricanes. *J. Climate,* **5,** 435–453.

——, and Coauthors, 2008: A reanalysis of the 1911–20 Atlantic hurricane database. *J. Climate,* **21,** 2138–2168.

Leroux, S., and N. Hall, 2009: On the relationship between African easterly waves and the African easterly jet. *J. Atmos. Sci.,* **66,** 2303–2316.

Lian, T., and D. Chen, 2012: An evaluation of rotated EOF analysis and its application to tropical Pacific SST variability. *J. Climate,* **25,** 5361–5373.

Lindzen, R. S., and A. V. Hou, 1988: Hadley circulations for zonally averaged heating centered off the equator. *J. Atmos. Sci.,* **45,** 2416–2427.

Maloney, E. D., and D. L. Hartmann, 2000: Modulation of hurricane activity in the Gulf of Mexico by the Madden–Julian oscillation. *Science,* **287,** 2002–2004.

Marshall, J., and Coauthors, 2001: North Atlantic climate variability: Phenomena, impacts and mechanisms. *Int. J. Climatol.,* **21,** 1863–1898.

Mitas, C. M., and A. Clement, 2005: Has the Hadley cell been strengthening in recent decades? *Geophys. Res. Lett.,* **32,** L03809, doi:10.1029/2004GL021765.

Montgomery, M. T., Z. Wang, and T. J. Dunkerton, 2010: Coarse, intermediate and high resolution numerical simulations of the transition of a tropical wave critical layer to a tropical storm. *Atmos. Chem. Phys.,* **10,** 10 803–10 827.

——, and Coauthors, 2012: The Pre-Depression Investigation of Cloud-Systems in the Tropics (PREDICT) Experiment: Scientific basis, new analysis tools, and some first results. *Bull. Amer. Meteor. Soc.,* **93,** 153–172.

Neelin, J. D., O. Peters, and K. Hales, 2009: The transition to strong convection. *J. Atmos. Sci.,* **66,** 2367–2384.

Nolan, D. S., E. D. Rappin, and K. A. Emanuel, 2007: Tropical cyclogenesis sensitivity to environmental parameters in radiative–convective equilibrium. *Quart. J. Roy. Meteor. Soc.,* **133,** 2085–2107.

Oort, A. H., and E. M. Rasmusson, 1970: On the annual variation of the monthly mean meridional circulation. *Mon. Wea. Rev.,* **98,** 423–442.

——, and J. J. Yienger, 1996: Observed interannual variability in the Hadley circulation and its connection to ENSO. *J. Climate,* **9,** 2751–2767.

Pu, B., and K. H. Cook, 2012: Role of the West African westerly jet in Sahel rainfall variations. *J. Climate,* **25,** 2880–2896.

Pytharoulis, I., and C. D. Thorncroft, 1999: The low-level structure of African easterly waves in 1995. *Mon. Wea. Rev.,* **127,** 2266–2280.

Raymond, D. J., 2000: Thermodynamic control of tropical rainfall. *Quart. J. Roy. Meteor. Soc.,* **126,** 889–898.

——, and C. López Carrillo, 2011: The vorticity budget of developing Typhoon Nuri (2008). *Atmos. Chem. Phys.,* **11,** 147–163.

Reed, R. J., 1988: On understanding the meteorological causes of Sahelian drought. *Persistent Meteo-Oceanographic Anomalies and Teleconnections,* C. Chagas and G. Puppi, Eds., Pontificae Academiae Scientiarum, 179–213.

Rozoff, C. M., W. H. Schubert, B. D. McNoldy, and J. P. Kossin, 2006: Rapid filamentation zones in intense tropical cyclones. *J. Atmos. Sci.,* **63,** 325–340.

Saha, S., and Coauthors, 2010: The NCEP Climate Forecast System Reanalysis. *Bull. Amer. Meteor. Soc.,* **91,** 1015–1057.

Shapiro, L. J., 1982: Hurricane climatic fluctuations. Part II: Relation to large-scale circulation. *Mon. Wea. Rev.,* **110,** 1014–1023.

Smith, T. M., R. W. Reynolds, T. C. Peterson, and J. Lawrimore, 2008: Improvements to NOAA's historical merged land–ocean surface temperature analysis (1880–2006). *J. Climate,* **21,** 2283–2296.

Stachnik, J. P., and C. Schumacher, 2011: A comparison of the Hadley circulation in modern reanalyses. *J. Geophys. Res.,* **116,** D22102, doi:10.1029/2011JD016677.

Swanson, K. L., 2008: Nonlocality of Atlantic tropical cyclone intensities. *Geochem. Geophys. Geosyst.,* **9,** Q04V01, doi:10.1029/2007GC001844.

Thorncroft, C., and K. Hodges, 2001: African easterly wave variability and its relationship to Atlantic tropical cyclone activity. *J. Climate,* **14,** 1166–1179.

Thorncroft, C. D., N. Hall, and G. Kiladis, 2008: Three-dimensional structure and dynamics of African easterly waves. Part III: Genesis. *J. Atmos. Sci.,* **65,** 3596–3607.

Vecchi, G. A., and B. J. Soden, 2007: Effect of remote sea surface temperature change on tropical cyclone potential intensity. *Nature,* **450,** 1066–1070.

——, K. L. Swanson, and B. J. Soden, 2008: Whither hurricane activity? *Science,* **322,** 687–689.

Ventrice, M. J., C. D. Thorncroft, and M. A. Janiga, 2012: Atlantic tropical cyclogenesis: A three-way interaction between an African easterly wave, diurnally varying convection, and a convectively coupled atmospheric Kelvin wave. *Mon. Wea. Rev.,* **140,** 1108–1124.

Vimont, D. J., and J. P. Kossin, 2007: The Atlantic meridional mode and hurricane activity. *Geophys. Res. Lett.,* **34,** L07709, doi:10.1029/2007GL029683.

Waliser, D. E., and R. C. J. Somerville, 1994: Preferred latitudes of the intertropical convergence zone. *J. Atmos. Sci.,* **51,** 1619–1639.

Wang, Z., 2012: Thermodynamic aspects of tropical cyclone formation. *J. Atmos. Sci.,* **69,** 2433–2451.

——, M. T. Montgomery, and T. J. Dunkerton, 2009: A dynamically-based method for forecasting tropical cyclogenesis location in the Atlantic sector using global model products. *Geophys. Res. Lett.,* **36,** L03801, doi:10.1029/2008GL035586.

——, ——, and ——, 2010a: Genesis of pre–Hurricane Felix (2007). Part I: The role of the wave critical layer. *J. Atmos. Sci.,* **67,** 1711–1729.

——, ——, and ——, 2010b: Genesis of pre–Hurricane Felix (2007). Part II: Warm core formation, precipitation evolution, and predictability. *J. Atmos. Sci.,* **67,** 1730–1744.

——, ——, and C. Fritz, 2012: A first look at the structure of the wave pouch during the 2009 PREDICT–GRIP dry runs over the Atlantic. *Mon. Wea. Rev.,* **140,** 1144–1163.

Webster, P. J., and H. Chang, 1988: Equatorial energy accumulation and emanation regions: Impacts of a zonally varying basic state. *J. Atmos. Sci.,* **45,** 803–829.

Xue, Y., T. M. Smith, and R. W. Reynolds, 2003: Interdecadal changes of 30-yr SST normals during 1871–2000. *J. Climate,* **16,** 1601–1612.

Yin, X., A. Gruber, and P. Arkin, 2004: Comparison of the GPCP and CMAP merged gauge–satellite monthly precipitation products for the period 1979–2001. *J. Hydrometeor.,* **5,** 1207–1222.

Zebiak, S. E., 1993: Air–sea interaction in the equatorial Atlantic region. *J. Climate,* **6,** 1567–1586.